

## Article

# Study of Influence Factors in the Evaluation of the Performance of a Photocatalytic Fibre Reactor (TiO<sub>2</sub>/SiO<sub>2</sub>) for the Removal of Organic Pollutants from Water

Juan C. García-Prieto <sup>1</sup>, Luis A. González-Burciaga <sup>2</sup>, José B. Proal-Nájera <sup>2</sup> and Manuel García-Roig <sup>1,\*</sup>

<sup>1</sup> Centro de Investigación y Desarrollo Tecnológico del Agua, Universidad de Salamanca, Campo Charro s/n, 37080 Salamanca, Spain; jcgarcia@usal.es

<sup>2</sup> CIIDIR-Unidad Durango, Instituto Politécnico Nacional, Calle Sigma 119, Fracc. 20 de Noviembre II, Durango 34220, Mexico; luis.gonzalez.iq@gmail.com (L.A.G.-B.); jproal@ipn.mx (J.B.P.-N.)

\* Correspondence: mgr@usal.es

**Abstract:** The performance of a photocatalytic fibre reactor (UBE Chemical Europe), made of cartridges of fine particles of TiO<sub>2</sub> dispersed within silicon fibres and irradiated by ultraviolet light, for the removal of organic pollutants from synthetic waters was evaluated. In the sensitivity analysis carried out, the factors catalytic surface area, fibre state, temperature and initial substrate concentration were studied using 4-chlorophenol as a test compound. The percentage of titanium in the fibre remained practically invariable after a series of experiments and cleaning procedures. Furthermore, the kinetics of removal of pyrene, phenol, 4-chlorophenol and bisphenol A (BPA) from water were evaluated by means of HPLC, UV-absorption and fluorescence techniques. Kinetic operational parameters were determined from a mathematical model proposed by Langmuir–Hinshelwood. Results show that catalytic surface, initial substrate concentration and temperature directly affect the degradation rate of organic compounds, whereas fibre state does not have a significant effect on that. It is proposed that removal of organic compounds from water mainly depends on the adsorption of the specific pollutant on the photocatalytic fibre and on the physical diffusion of the substrate towards the photocatalytic TiO<sub>2</sub> active sites on the fibre, with the heterogeneous phase reaction prevailing over the homogeneous phase reaction.

**Keywords:** photocatalysis; organic compounds; photocatalytic glass fibre; photodegradation; adsorption; heterogeneous phase; homogeneous phase



**Citation:** García-Prieto, J.C.; González-Burciaga, L.A.; Proal-Nájera, J.B.; García-Roig, M. Study of Influence Factors in the Evaluation of the Performance of a Photocatalytic Fibre Reactor (TiO<sub>2</sub>/SiO<sub>2</sub>) for the Removal of Organic Pollutants from Water. *Catalysts* **2022**, *12*, 122. <https://doi.org/10.3390/catal12020122>

Academic Editors: Aadesh P. Singh and Matthias Vandichel

Received: 16 December 2021

Accepted: 17 January 2022

Published: 20 January 2022

**Publisher's Note:** MDPI stays neutral with regard to jurisdictional claims in published maps and institutional affiliations.



**Copyright:** © 2022 by the authors. Licensee MDPI, Basel, Switzerland. This article is an open access article distributed under the terms and conditions of the Creative Commons Attribution (CC BY) license (<https://creativecommons.org/licenses/by/4.0/>).

## 1. Introduction

Many methods for degrading organic compounds in water and wastewater have been developed during the last decades in order to reduce their effects on the environment and human health [1]. These compounds are classified as bio-recalcitrant and not biodegradable organic pollutants since they cannot be removed by traditional physical-chemical and biological treatment technologies [2,3].

Heterogenous photocatalysis (HPC) has become the most distinctive, popular, effective and promising treatment technique for the removal of recalcitrant contaminants, such as organic pollutants, in wastewater [4]. The mechanism of HPC consists of the capability of photon excitation on a semiconductor surface. Photon incidence causes electrons migration from valence band to conduction band generating hole/electron pairs (h<sup>+</sup>/e<sup>-</sup>). Valence-band holes are powerful oxidants while valence conduction electrons are powerful reductants. Migrated electrons hydrolyse water molecules to generate hydroxyl radicals (•OH) in situ, which are extremely reactive and strong oxidizing agents (•OH, oxidative potential of 2.8 eV), and can lead to further reactions generating harmless products such as CO<sub>2</sub> and H<sub>2</sub>O [5–7].

A wide variety of compounds can be used as semiconductors in photocatalysis (e.g., Si,  $\text{WO}_3$ , ZnS,  $\text{SnO}_2$ ,  $\text{Fe}_2\text{O}_3$ ,  $\text{Fe}_3\text{O}_4$ , ZnO, CdS, ZnS, SrTiO<sub>3</sub>, WSe<sub>2</sub> and TiO<sub>2</sub> (rutile or anatase)). These are characterized by a filled valence band and an empty conduction band [8–11]. Over the past decades, TiO<sub>2</sub> has been widely used to treat water pollutants due to its low cost, good stability, and high photocatalytic activity. Furthermore, it is biologically inert and resistant to chemical corrosion and can be used at ambient temperature and pressure [12–15]. Heterogeneous photocatalysis (HPC) is used to avoid the limitation of separating TiO<sub>2</sub> powder from the suspension after cleaning wastewater [16]. Other problems associated with the TiO<sub>2</sub> suspended particles are: (a) ensuring that light has effective access to the photocatalyst; (b) photocatalyst suspensions exhibit significant light scattering and absorption phenomenon making homogeneous external illumination of the suspension difficult [17]. Moreover, different immobilizations of semiconductors on solid supports have been studied [18–23] to increase the adsorption of pollutants and photocatalytic activity [24,25]. Often, semiconductors are loaded with metal to improve the efficiency of the photocatalytic process [26–29].

Many materials have been developed to avoid thermomechanical stress at the interface between catalyst layer and support. The catalysts (TiO<sub>2</sub>) are deposited in surface layers by means of different techniques such as chemical vapour deposition [30], slip cast [31], ceramics [32], dry processing [18], coating methods and thermal chemical reactions [33] and inorganic fibres [19].

Practical application of metal oxide semiconductors as photocatalysts requires immobilization of the photocatalyst in a fixed-bed reactor configuration that allows the continuous use (commercial use) of the photocatalyst for treating aqueous or gaseous effluent streams by eliminating the need for post-process filtration. The fibre photocatalytic fixed bed reactors show advantages on the TiO<sub>2</sub> suspended particles due to its higher uniformity and the greater extent of light propagation towards the fibre, the greater level of the refracted light absorption by the TiO<sub>2</sub> coating, and the ability of the chemical substrates to diffuse towards the TiO<sub>2</sub> coating. It also shows great strength and stability against acidic and alkaline effluents without suffering degradation. However, supported photocatalysts have reduced surface areas and need to have an unobscured path between the photocatalyst and the light source [34]. Another important operational parameter is the power of the UV-C ultraviolet irradiation and, therefore, the rate of photocatalytic activation and the formation of the electron-hole pair are strongly influenced by the power of the UV-C irradiant light [35,36]. It is also well known, photocatalytic oxidation is reasonably efficient when the concentration of organic compounds in the solution is low to moderate, but it fails to purify aqueous solutions with a high concentration of total organic carbon [37], the photocatalytic activity being strongly dependent on its phase structure, crystalline size, specific surface areas, and pore structure of the photocatalyst [38].

In this article, organic compounds degradation by heterogeneous photocatalysis with TiO<sub>2</sub> supported on SiO<sub>2</sub> fibre in an industrial photoreactor (UBE Chemical Ltd., Tokyo, Japan) is studied. With this photoreactor, previous works have been carried out on wastewater disinfection and on degradation of organic compounds [39–45]. The novelty of this work with respect to the aforementioned studies, focused mainly on the degradation kinetics of organic compounds, lies in the fact of considering not only said kinetic study but also the physico-chemical effects of the adsorption of these compounds in the surface of the catalyst, of the water flow rate and of the stability of the photocatalyst, when adding other substances such as H<sub>2</sub>O<sub>2</sub> (Fenton effect), on the performance and the kinetics of the process. In this study, the technology developed by the group of Ishikawa [18,19] was used for replacing conventional TiO<sub>2</sub>-coated support with a new TiO<sub>2</sub> support material which was implemented and checked in a fixed bed reactors pilot plant supplied by UBE Chemical Co. Therefore, the aim of this work was to assess the process performance of a photocatalytic reactor which incorporates as catalyst a fibrous ceramic silica—TiO<sub>2</sub> composite. Assessment is focused on three fundamental aspects: (1) system modularization and kinetics, (2) fibre stability and (3) system feasibility and effectiveness treating organic compounds. Model

organic compounds used in this study were polycyclic aromatic hydrocarbon (PAH), such as pyrene, and phenolic compounds, such as phenol, 4-chlorophenol and bis-phenol A (BPA). The latter (BPA) is one of the known as endocrine disrupting compounds (EDC's) which have a special interest since they can cause adverse effects by interfering with the body's hormones or chemical messengers at very low concentrations [46]. The European Directive 2008/105/EC on Environmental Quality Standards established, in Annex I, limits on concentrations of these priority substances [47].

## 2. Results

### 2.1. Kinetic Modelling of Photolytic and Photocatalytic Degradation Processes

The photocatalytic degradation rates of the pollutants studied have been fitted by the Langmuir-Hinshelwood (L-H) kinetic model [48]. The analysis of the data, according to this model, assumes that the reactions are superficial ( $\Theta$ ), which is accepted [49]. The reaction rate is then defined according to the equation:

$$v = -\frac{dC}{dt} = k\Theta = \frac{k K C}{1 + K C + \sum_{i=1}^m K_i C_i} \quad (i = 1, \dots, m) \quad (1)$$

where  $\Theta$  is the surface coverage,  $i$  is the number of intermediates formed during degradation (water is also included in the sum),  $k$  is the reaction constant,  $K$  is the adsorption constant of the organic compound on the catalyst,  $C$  is the instantaneous concentration of the organic compound,  $C_i$  is the instantaneous concentration of each intermediate (type  $i$ ) that may be formed and  $K_i$  is its adsorption constant on the catalyst. If it is considered that the concentration of reaction intermediates is always low ( $C_i \ll C$ ), which is admissible as long as the initial concentration of the organic compound is small [50], and given that  $C < 0.15$  g/L, for the organic compounds studied, the sum corresponding to the intermediates can be disregarded, obtaining again the equation:

$$v = -\frac{dC}{dt} = \frac{k K C}{1 + K C} \quad (2)$$

Integrating the above differential equation gives the expression:

$$t = \frac{1}{k} (C_0 - C_t) + \frac{1}{k K} \ln \left( \frac{C_0}{C_t} \right) \quad (3)$$

A classical approach is to consider that the initial pollutant concentration is not very large and the adsorption equilibrium constant usually has a sufficiently small value, so that the term  $1 + KC$  can be approximated to 1, since  $1 \gg KC$ :

$$v = -\frac{dC}{dt} = k K C = k_{FC} C \quad (4)$$

where  $k_{FC}$  is the operational constant expressed as the product of the rate constant and the adsorption equilibrium constant ( $k_{FC} = kK$ ). The integral of Equation (4) relates the concentration of organic pollutants present in the mixture to the time elapsed in the photocatalytic process:

$$[C] = [C]_0 e^{-k_{FC} t} \quad (5)$$

Which in logarithmic form looks like:

$$\ln \left( \frac{C_0}{C_t} \right) = k_{FC} t \quad (6)$$

The treatment time can be replaced by the illumination time during photocatalysis, giving the relationship between the pollutant concentration and the illumination time ( $t$ ). Accordingly, the slope of the graph of  $\ln(C_0/C_t)$  versus  $t$  gives the operational constant ( $k_{op}$ ) or first order kinetic constant.

On the other hand, organic compounds can be photolytically decomposed by two parallel or competitive reactions that would fit the equation:

$$v = -\frac{dC}{dt} = k_1 \Theta + k_2 C \quad (7)$$

Likewise,  $k_1$  is the rate constant corresponding to the photocatalytic process and  $k_2$  is the rate constant corresponding to the photochemical process. Taking into account the above considerations (Equation (4)) that the product  $KC$  is much smaller than unity and taking out the common factor we would obtain the equation:

$$v = -\frac{dC}{dt} = (k_1 K + k_2) C \quad (8)$$

Equation corresponding to kinetics of first order, where the product  $k_1 K$  would be equal to a constant corresponding to the photocatalytic process, which we will call  $k_{FC}$ , while  $k_2$ , which is the rate constant corresponding to the photolytic process, we will call  $k_{FQ}$ , from now on. This would leave the equation:

$$v = -\frac{dC}{dt} = (k_{FC} + k_{FQ}) C \quad (9)$$

Whose integrated equation assumes a monoexponential decay of  $[C]$ :

$$[C] = [C]_0 e^{-(k_{FC} + k_{FQ})t} \quad (10)$$

$$[C] = [C]_0 e^{-k_{op}t} \quad (11)$$

With the reactor operational constant ( $k_{op}$ ) being equal to the sum of the two constants

## 2.2. Kinetic Study of the Influence of Catalyst Surface on the Degradation of Pollutant

The photolytic degradation of phenol and its simple halogenated derivatives has been extensively studied [51]. The model compound, 4-chlorophenol, will be degraded by two parallel reactions, the photocatalytic pathway and the photolytic pathway. To carry out the study, six experiments were carried out, four of them varying the amount of cone-shaped catalyst cartridges to study the photocatalytic pathway, and another two trials, in order to study only the photolytic pathway, one of them without photocatalyst and with UV-C lamp, and the other experiment irradiating with UV-C ultraviolet light, but replacing the photocatalytic fibre with glass wool.

Figure 1 below shows the fits of the competitive monoexponential model presented for the study of the decrease in 4-chlorophenol concentration as a function of time for the four photocatalytic experiments performed. The goodness of the fits is represented by values very close to 1 of the Coefficient of Determination ( $0.9992 < R^2 < 0.9997$ ) and very small of the Mean Squared Error ( $1.49 \times 10^{-4} < \text{MSE} < 5.89 \times 10^{-4}$ ).

Table 1 below shows the kinetic constants of the system,  $k_{op} = k_{FC} + k_{FQ}$  and  $k_{FQ}$ , obtained for each experiment and determined by non-linear regression fitting of the substrate concentration *versus* time data to the model defined in Equations (10) and (11), as well as the values of the photolytic ( $k_{FQ}$ ) and photocatalytic ( $k_{FC}$ ) constants calculated from the aforementioned approximations.

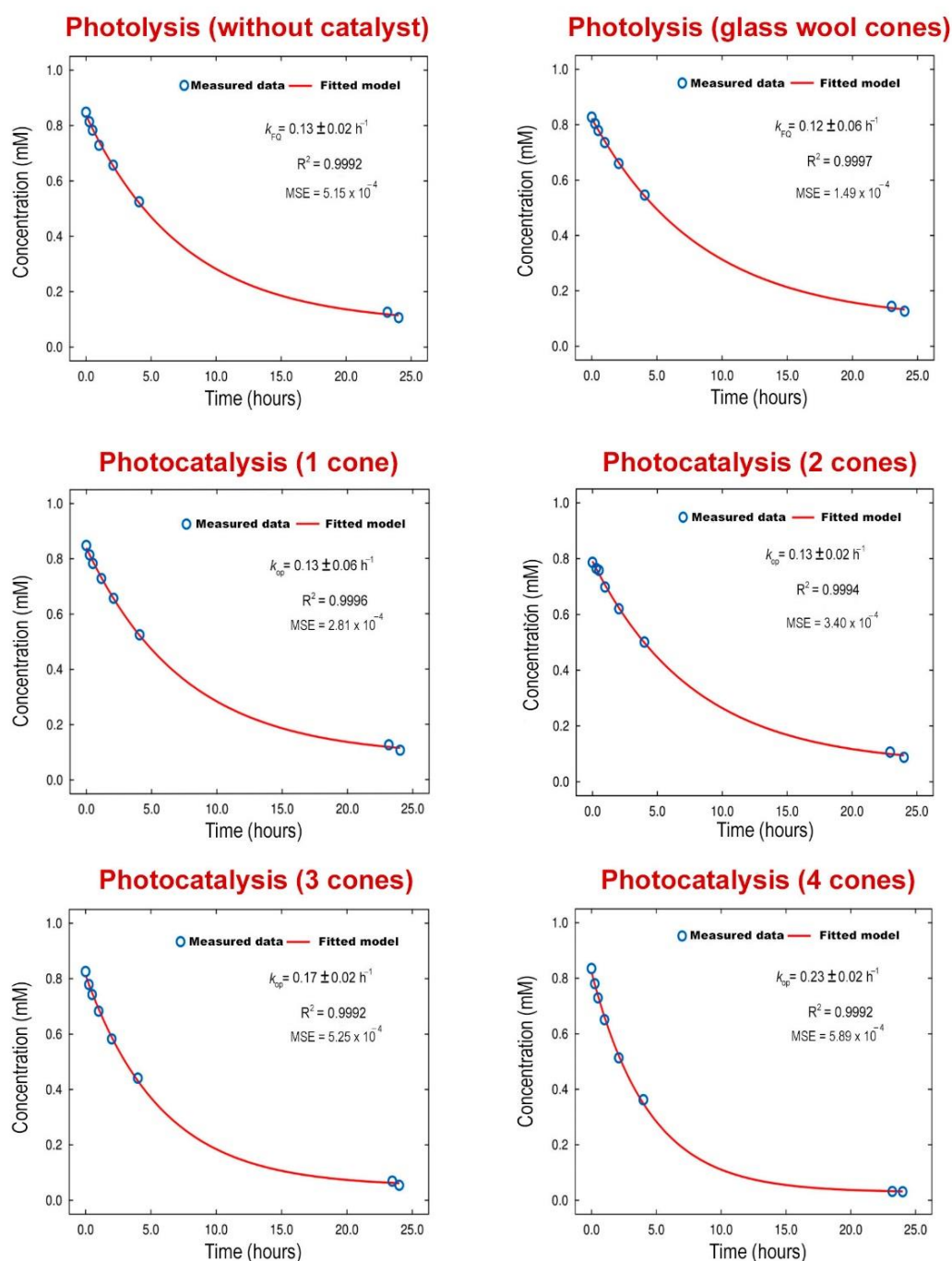


**Figure 1.** Influence of the photocatalyst surface on the degradation of 4-chlorophenol at  $Q = 2000$  L/h and  $T = 20 \pm 1$  °C.

**Table 1.** Rate constants of the photolytic and photocatalytic process.

Number of Cones	0	1	2	3	4
$k_{op} = k_{FC} + k_{FQ}$ ( $h^{-1}$ )		$0.13 \pm 0.06$	$0.13 \pm 0.02$	$0.17 \pm 0.02$	$0.23 \pm 0.02$
Photolysis $k_{FQ}$ ( $h^{-1}$ )	$0.13 \pm 0.02$	$0.129^*$	$0.126^*$	$0.123^*$	$0.12 \pm 0.06$
** Photocatalysis $k_{FC}$ ( $h^{-1}$ )		0	0.01	0.05	0.11

\* The values without confidence limits are calculated by linear regression from the values obtained by fitting the kinetic data to the model of Equation (5) in the photolytic effect (Figure 2). \*\* The values of the photocatalytic rate constant ( $k_{FC}$ ) are calculated by the difference between the values of the operational rate constant ( $k_{op} = k_{FC} + k_{FQ}$ ) and the values of the photolytic rate constant ( $k_{FQ}$ ).

Figure 2 shows the influence of each of these effects on the degradation of 4-chlorophenol:

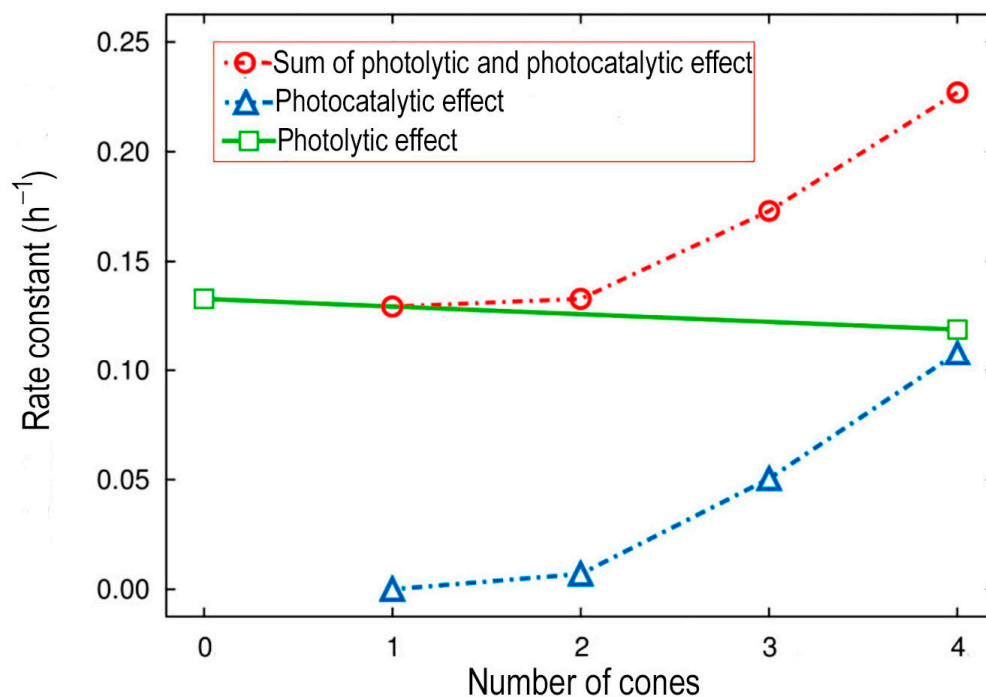


**Figure 2.** Variation of the rate constant as a function of photocatalyst surface area in the degradation of 4-chlorophenol at  $Q = 2000$  L/h and  $T = 20 \pm 1$  °C.

The results show the positive effect of increasing the number of photocatalytic cartridges on the degradation of the organic compound, i.e., increasing the photocatalytic active surface area (number of active  $\text{TiO}_2$  sites) increases the rate of degradation of the substrate. Thus, the generation of hydroxyl radicals ( $\bullet\text{OH}$ ) leads to an increase in the degradation rate of organic compounds, as has been observed by other authors [8]. However, the variation of  $k_{FC}$  with the number of cones does not follow a linear dependence, as one would expect when assuming that the photocatalytic operational constant ( $k_{FC}$ ) is expressed as the product of the photocatalytic rate constant and the equilibrium constant of the adsorption process ( $k_{FC} = k_1K$ ), but rather the degradation constant increases exponentially as the catalyst area increases proportionally. This could be due to various factors such as the adsorption of the pollutant or some of the by-products formed during its degradation on the surface of the catalyst, causing a loss of the effective capacity of the photocatalyst, or to operational flow modifications as a consequence of modifying the reaction volume, by modifying the number of cones, which produces a variation in the contact time of the pollutant on the surface of the photocatalyst.

### 2.3. Kinetic Analysis of the Effect of the Contact Time of the Pollutant with the Catalyst Surface

An important parameter to take into account in photocatalytic processes is the residence time or the time that each unit of fluid will be exposed to the catalyst and radiation as it passes through the reactor since the residence time in the reactor must be at least equal to the time required to carry out the adsorption-desorption processes necessary to favour the reaction of the adsorbed substance on the surface of the catalyst.

The operational condition controlling the contact time between the adsorbed species and the adsorbent (photocatalytic fibre) is the flow rate. To carry out the flow rate study, four experiments were carried out with four new photocatalytic fibre cartridges and the clean quartz tube with similar initial concentrations of 4-chlorophenol at temperature  $25 \pm 1$  °C and with flow rates of 500, 1000, 1500 and 2000 L/h. Table 2 shows the values of the operational rate constants ( $k_{op} = k_{FC} + k_{FQ}$ ) for each of the flow rates studied, indicating

also the hydraulic retention time ( $T_R$ ), which is defined as the ratio between the volume of the reactor ( $V_R$ ) and the flow rate ( $Q$ ) that flows through this volume:

$$T_R = \frac{V_R}{Q} \quad (12)$$

Reactor volume ( $V_R$ ) measured experimentally without catalyst 3.5 dm<sup>3</sup> and with catalyst 3.1 dm<sup>3</sup>.

**Table 2.** Rate constants of the photolysis and photocatalysis process as a function of flow rate (contact time).

Flow Rate (L/h)	500	1000	1500	2000
$k_{op} = k_{FC} + k_{FQ}$ (h <sup>-1</sup> )	0.22 ± 0.08	0.31 ± 0.09	0.32 ± 0.09	0.28 ± 0.09
$T_R$ (minutes)	0.37	0.19	0.12	0.09

Figure 3 shows the operational rate constant *versus* the flow rate (lower axis) and the contact time (upper axis) within the photocatalytic reactor.

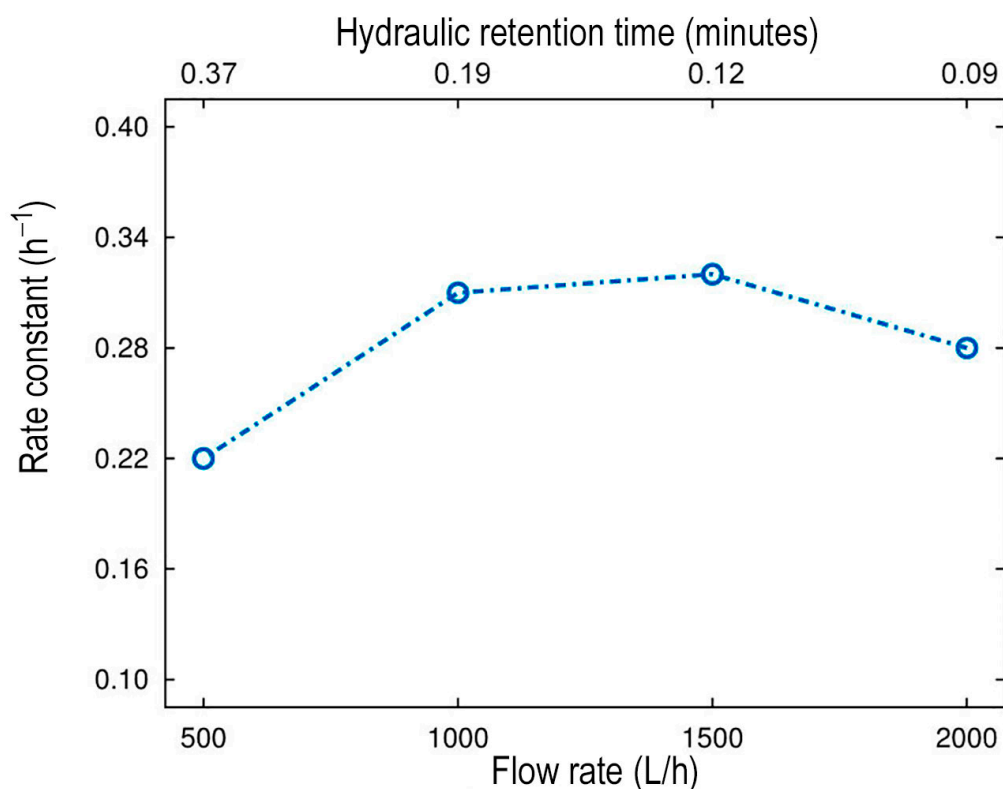


**Figure 3.** Variation of the operational rate constant ( $k_{op}$ ) as a function of flow rate (lower axis) and contact time (upper axis) in the degradation of 4-chlorophenol at  $C = 0.8$  mM and  $T = 25 \pm 1$  °C.

Considering the approximation that the observed photolytic effect is similar at all flow rates studied, since the fundamental parameter on which it depends is the intensity of the lamp and the energy transfer (UV-C radiation) is faster than the matter transfer operations, it is observed that initially the reaction rate increases with time, since the transfer of matter to the catalyst surface is the rate limiting step, so the reaction rate increases with flow rate. As the flow rate increases, the reaction starts to be controlled by surface kinetics and the flow rate affects the reaction rate less, at which point the reaction rate could be considered to be independent of the flow rate. At high flow rates, the contact time may be too short for the transfer of matter from the liquid phase to the surface of the photocatalytic fibre, in which case surface phenomena would limit the reaction rate, which would decrease with

increasing flow rate. As can be seen in Figure 3, the optimum hydraulic retention time is between 0.1 and 0.2 min, which corresponds to flow rates between 1000 and 1500 L/h.

#### 2.4. Kinetic Study of the Effect of the Initial Concentration of the Pollutant

The overall kinetics of the process will depend on the matter transfer operations in the adsorption-desorption stage of the organic compound and on the surface rate on the photocatalyst surface, with the availability of active sites being a limiting factor in the rate of degradation of the compound [52]. Surface phenomena have a great influence, so that the reaction rate at low concentrations increases significantly due to the large number of free active sites, but as the pollutant concentration increases, the reaction rate follows an asymptotic behaviour because the catalyst surface becomes saturated, so that an increase in the substrate concentration hardly increases the reaction rate. This phenomenon occurs when the catalyst sites are occupied either by the reactants (at high concentrations) or by the reaction products. A model that interprets this behaviour well is the Langmuir–Hinshelwood model.

To study the influence of the initial substrate concentration, increasing concentrations of 4-chlorophenol between 0.1 and 2.0 mM were studied. For this purpose, four experiments were carried out under the usual conditions, this time with a new series of four photocatalytic cartridges. The recirculation flow rate was 2000 L/h, the volume of the feed tank was 50 L, the temperature was maintained at  $25 \pm 1$  °C, and the recirculation time was 4 h. To reduce the influence of the effects of adsorption of the reactants and intermediates on the catalyst surface, initial degradation rates were measured in this study (Figure 4). The best fits of the experimental kinetic curves were to monoexponential models ( $R^2 = 0.9705$ – $0.9994$ ,  $MSE = 1.48 \times 10^{-4}$  –  $2.02 \times 10^{-3}$ ) and the corresponding values of  $v_0$  are shown in Figure 4 for the different 4-chlorophenol initial concentrations. The green dotted line marks the tangent to the curve whose slope represents—the initial reaction rate ( $-v_0$ ) and the black dashed line indicates the asymptotic value.

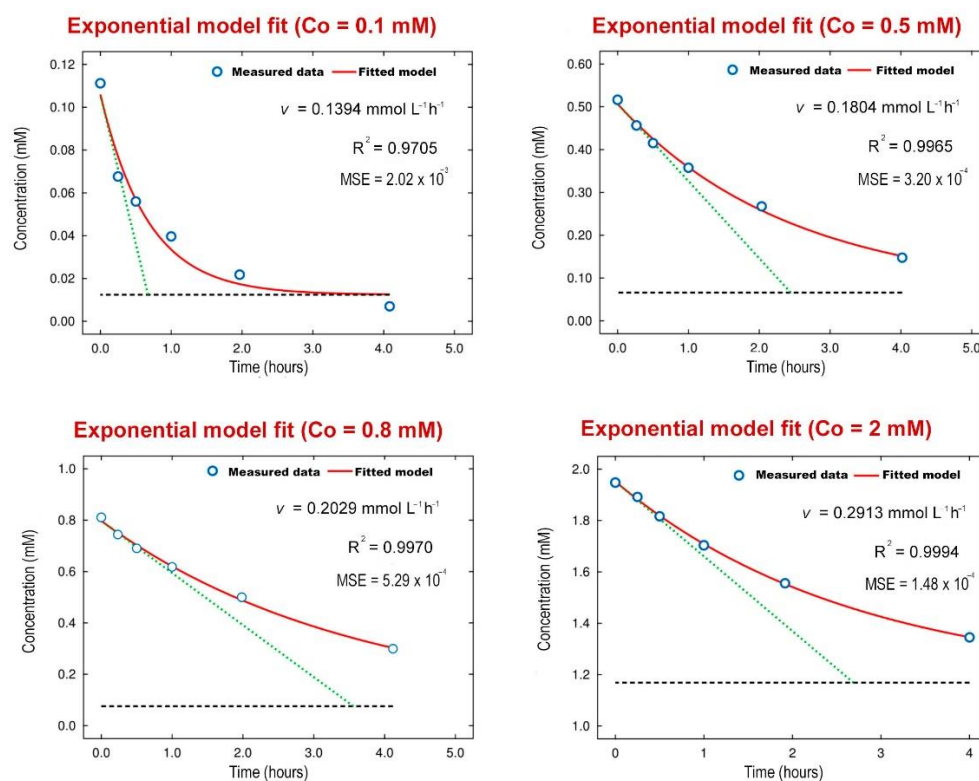


**Figure 4.** Initial degradation rates at different initial concentrations of 4-chlorophenol at  $Q = 2000$  L/h and  $T = 25 \pm 1$  °C.

The obtained initial rates ( $v_0$ ) for each initial concentration ( $C_0$ ) were fitted to the Langmuir–Hinshelwood differential equation. The fit to Equation (2), the Langmuir–Hinshelwood model, of the initial rates obtained *versus* initial substrate concentration is shown in Figure 5. The figure shows the estimates of the rate constant ( $k$ ), the adsorption equilibrium constant ( $K$ ) and the statistical quality of the fit ( $R^2 = 0.9501$ ,  $MSE = 1.22 \times 10^{-3}$ ).

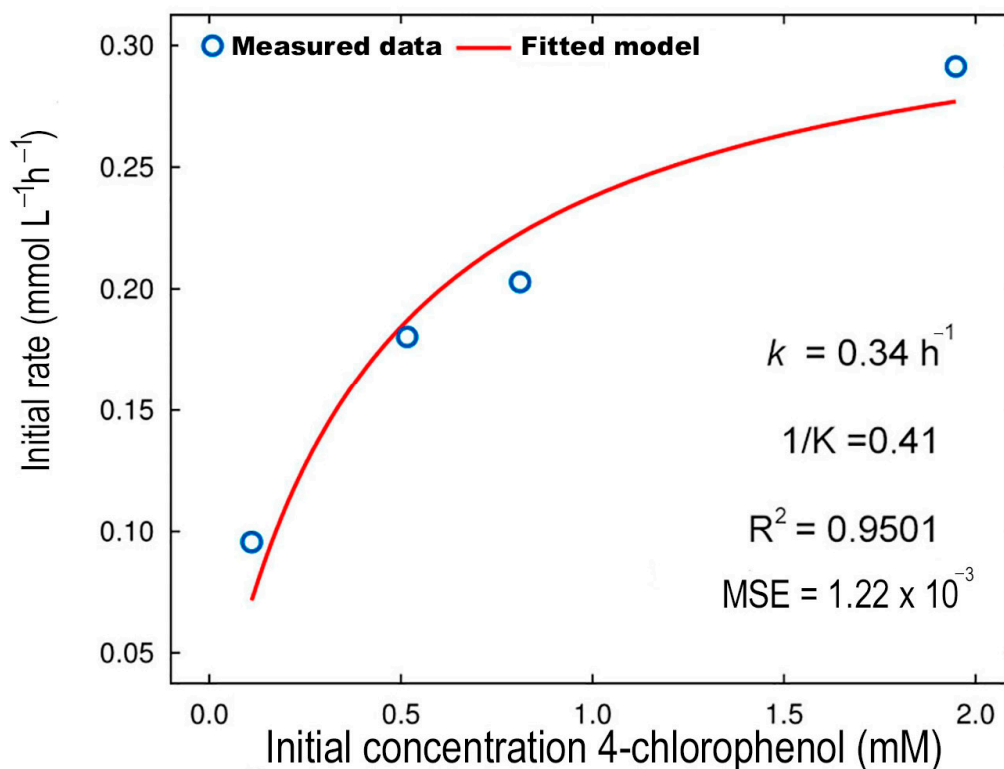


**Figure 5.** Fit to the Langmuir–Hinshelwood differential equation of the initial degradation rates of 4-chlorophenol *versus* initial substrate concentrations,  $Q = 2000$  L/h and  $T = 25 \pm 1$  °C.

The fitting of the integrated Langmuir–Hinshelwood velocity equation model (3) was carried out using the “QNFIT” program of the SIMFIT statistical package [53], based on the parameters, velocity constant and equilibrium constant, estimated previously. Table 3 below shows the values of the rate constant ( $k$ ), the adsorption equilibrium constant ( $K$ ), as well as the operational constant defined as the product of the two constants ( $k_{op} = k K$ ) for each concentration.

**Table 3.** Rate constants and equilibrium constant of 4-chlorophenol elimination at different initial concentrations.

Initial Concentrations	$k$ ( $\text{h}^{-1}$ )	$K$	$k_{op} = k$ ( $\text{h}^{-1}$ )
$C_0 = 0.1$ mM	$0.72 \pm 0.04$	1.56	1.13
$C_0 = 0.5$ mM	$0.47 \pm 0.09$	0.85	0.39
$C_0 = 0.8$ mM	$0.41 \pm 0.09$	0.85	0.34
$C_0 = 2$ mM	$0.24 \pm 0.09$	0.81	0.19

Under the conditions studied, it can be observed that the reaction rate constant ( $k$ ) decreases with increasing initial concentration of substrate. Likewise, a decrease in the adsorption equilibrium constant can be observed as a function of the initial concentration, which indicates that the surface reactions that have occurred on the surface of the photocatalytic fibre have had a great influence on the course of the reaction (heterogeneous phase) and on the reactions that may occur in the homogeneous phase during the course of the reaction. The surface coverage  $\Theta$  can be related to the substrate concentration  $C$  and the

apparent adsorption constant at equilibrium  $K$ , by means of Equation (1). The value of surface coverage will be between 0–1 since it indicates the ratio of occupied sites to total sites, tending to zero when all sites are free and to one when all sites are occupied [54]. Table 4 shows the values of the surface coverage.

**Table 4.** Surface coverage values as a function of initial substrate concentrations.

Initial Concentrations (mM)	0.1	0.5	0.8	2
Surface coverage $\Theta$	0.13	0.37	0.40	0.62

The results indicate that the adsorption of this pollutant, 4-chlorophenol, on the catalyst surface plays an essential role in the photocatalytic process. Therefore, at high substrate concentrations, there will be a high adsorption of 4-chlorophenol on the catalyst surface, so that the pollutant could cover the active sites of  $\text{TiO}_2$  preventing the passage of radiation, thus reducing the generation of the hole/electron pairs ( $h^+ / e^-$ ) and consequently the generation of the oxidising species ( $\bullet\text{OH}$ ). Therefore, a high pollutant concentration is in accordance with a low operational degradation rate constant. When the substrate concentration is low, there will be active sites available and more free photocatalytic surface, for the generation of oxidizing species and the degradation rate should increase (Table 3).

### 2.5. Influence of Temperature on the Photocatalytic Degradation of 4-Chlorophenol

Photocatalytic reactions are not very sensitive to thermal variations since activation occurs photonically and the rate constant is not so dependent on temperature as established by the Arrhenius law for conventional thermally activated reactions [55]. In photocatalytic reactions, temperature mainly affects the adsorption-desorption processes of reactants, intermediates and end products, so its effect depends on the surface characteristics of the photocatalytic fibre and the reactant to be decomposed [56].

In this work, it was decided to study the influence of temperature on the degradation of 4-chlorophenol in a temperature range between 17.5 °C and 25.0 °C measured in the reaction tank and controlled by means of a water cooler. The thermodynamic activation parameters (Eyring equation) of the photocatalytic decomposition reaction of 4-chlorophenol: enthalpy, entropy and Gibbs free energy of activation and the kinetic parameters (Arrhenius equation) frequency factor or pre-exponential factor and the activation energy of the reaction were calculated and shown in Table 5.

**Table 5.** Activation parameters for the degradation of 4-chlorophenol.

Pre-exponential factor ( $10^4 \text{ h}^{-1}$ )	$1.66 \pm 0.38$
Activation energy (kJ/mol)	$27 \pm 1$
Activation enthalpy (kJ/mol)	$25 \pm 1$
Activation entropy (J/mol.K)	$-172 \pm 5$
Activation Gibbs free energy at 298 K (kJ/mol)	$76 \pm 1$

These results indicate that the degradation efficiency is not significantly affected by increasing temperature, finding that is common in studies of photocatalytic processes. The low activation energy value obtained, i.e., the weak dependence of the degradation process on temperature, seems to indicate that the rate limiting step of the process should be the physical diffusion of the substrate towards the active sites on the surface of the photocatalytic  $\text{TiO}_2$  fibre. Positive values of the activation enthalpy indicate that the process is endothermic and positive values of the activation Gibbs energy indicate that the process is not spontaneous. The high negative entropy value indicates that the intermediate formed on the catalyst surface between the 4-chlorophenol and the free radicals ( $\bullet\text{OH}$ ) is more ordered than the reactant favouring its adsorption, this is in agreement with positive enthalpy and Gibbs free energy values.

### 2.6. Influence of Photocatalytic Fibre Condition on Pollutant Removal Rate

The influence of the state of the photocatalytic fibre was evaluated by comparing the conditions of the fibre before the start of each group of experiments and after the end of the experiments. To carry out these experiments, a study of the Titanium-Silicon surface ratio was carried out by means of scanning electron microscopy (SEM) with elemental microanalysis by X-ray scattering (EDX) (Figure 6). The variation of the operational rate constant of 4-chlorophenol degradation after each group of experiments was also studied to see the effect of the fibre coating on the degradation rate of the pollutant.

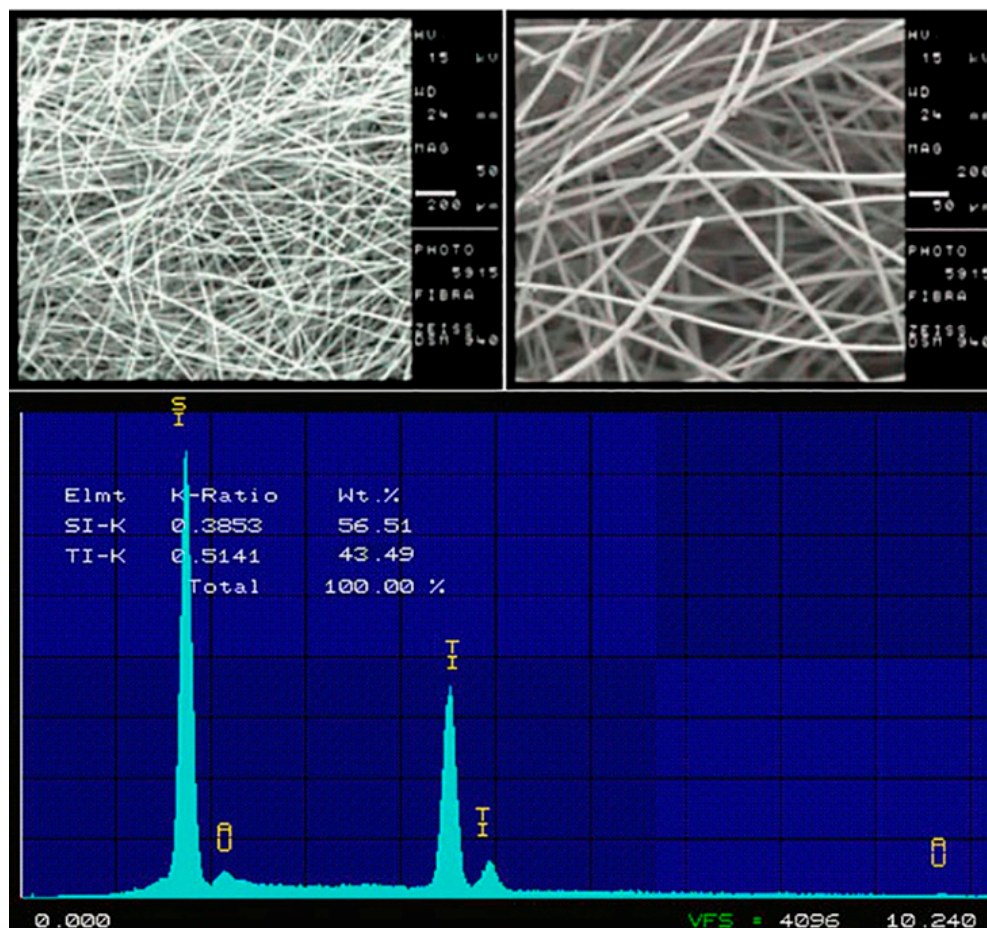


**Figure 6.** Structural characteristics of the original photocatalytic fibre before use. Surface analysis by SEM (upper panel) and by EDX elemental microanalysis (lower panel).

The coating of the photocatalytic fibre does not have such an influence on the degradation rate of the compound, because the results obtained for the operational rate constant were again of the same order of magnitude between the experiment with the clean fibre and the experiment with the coated fibre. It is also observed in the analysis of the fibre surface by EDX elemental microanalysis that there is not a change between the values of the surface titanium percentage of the unused fibre (43.49% Ti) and the coated fibre (43.60% Ti). This suggests that the generation of hydroxyl radicals on the surface of the photocatalyst is not affected by the possible fouling present on the fibre surface after several experiments. The new elements that appear in the EDX analysis may be due to ions in the milli-Q water, as well as iron and copper from the pilot plant construction material (the milli-Q water can be somewhat corrosive) (Figure 7).

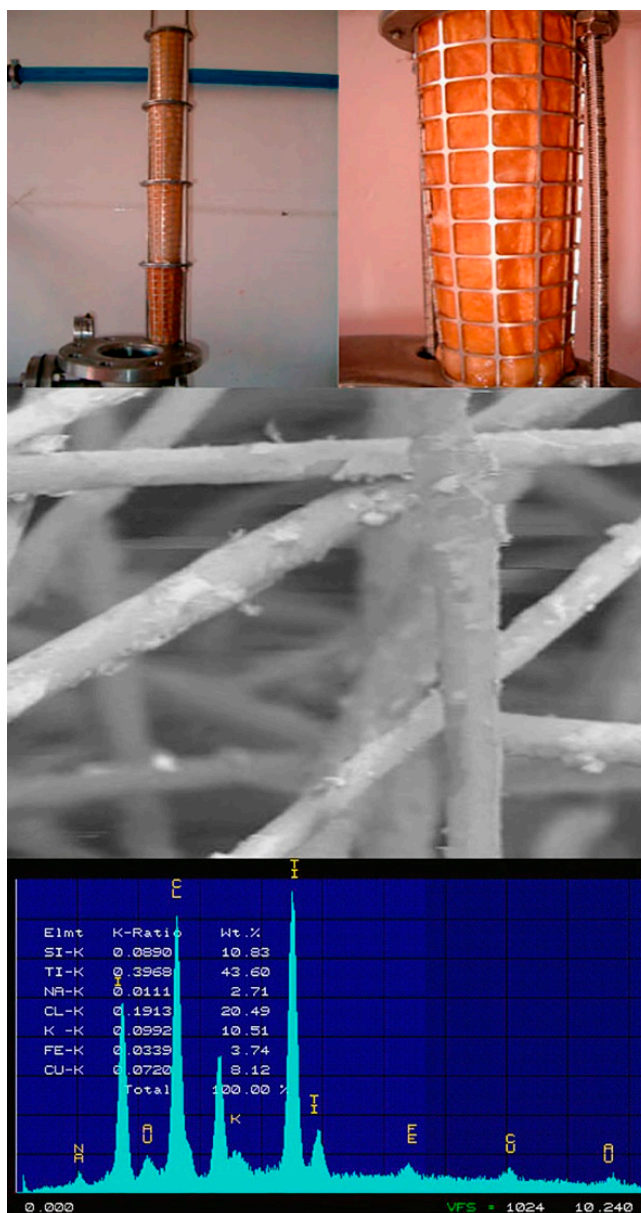


**Figure 7.** State of the photocatalytic fibre after 24 h of use in the photocatalytic degradation reaction of 0.8 mM 4-chlorophenol,  $Q = 2000$  L/h and temperature =  $20 \pm 1$  °C.

Countercurrent cleaning procedures with acids, bases and peroxides were performed, the fibre showed better appearance and loss of the reddish colouration with respect to the fibre used before the washing procedure, observing that the cleaning procedure by acid washing leaves a lighter colour on the fibre. However, a decrease in the percentage of surface titanium was observed after the washings. Due to the results obtained in the fibre washing study, it was decided to study the characteristics of the fibre when treated with acids, bases and peroxides. This study of the stability of the fibre is shown below.

### 2.7. Study of the Stability of the Photocatalytic Fibre against Acids, Bases and Peroxides

In order to study the stability of the photocatalytic fibre against acids (HCl) and bases (NaOH), the degradation suffered by the photocatalytic fibre was determined according to the method for determining soluble matter in bases and acid (basic and acid loss) described in the UNE-EN-12902 standard [57]. The results are shown in Figure 8.

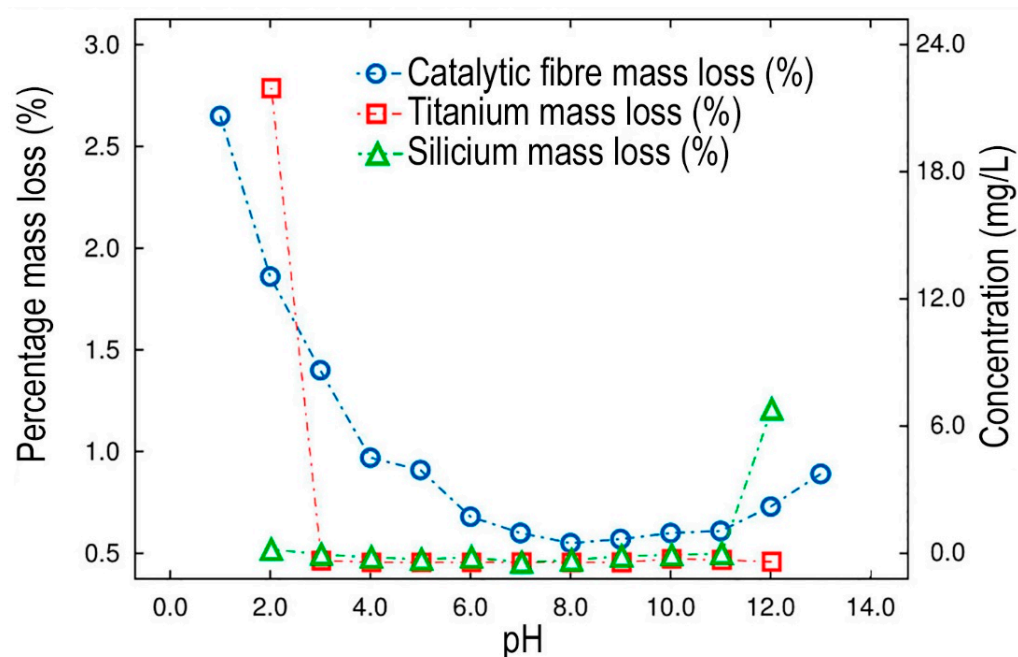


Figure 8. Stability of the photocatalytic fibre *versus* pH.

The study of fibre stability against acids and bases indicates that the fibre is stable with respect to pH, except at extreme pHs, with loss of titanium at very acidic pHs and loss of silicon at very basic pHs. On the other hand, it is observed that the fibre is less stable against peroxides (Figure 9), due to the fact that at high concentrations of peroxides, degradation of the fibre is observed due to loss of active surface (titanium). The use of the photo-Fenton effect to catalyse heterogeneous photocatalysis reactions with this photocatalyst material may be affected by the loss of surface titanium (Figure 9).

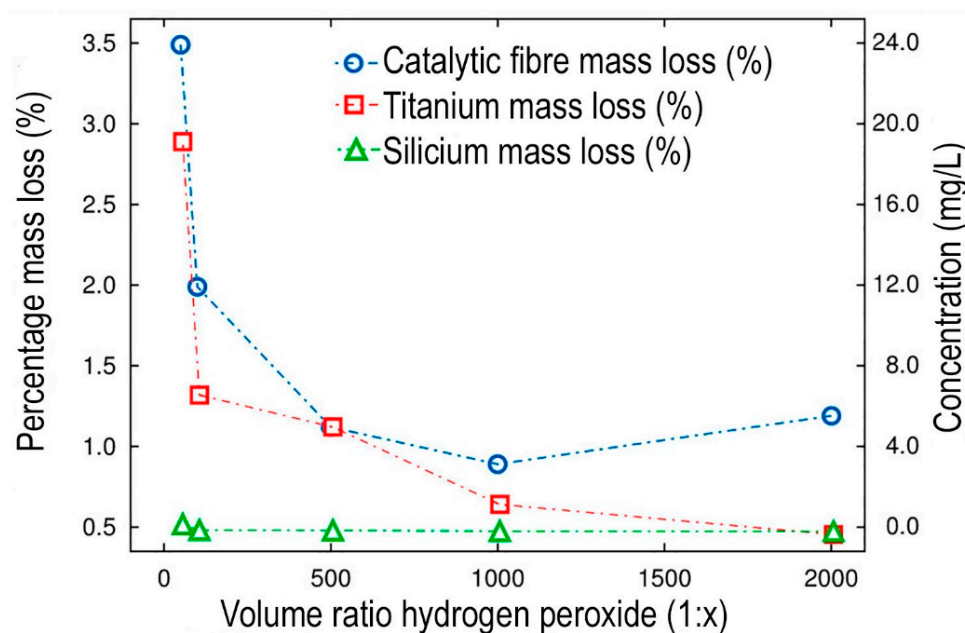


Figure 9. Stability of the photocatalytic fibre against hydrogen peroxide concentrations.

These results are consistent with those observed by Adan et al. [44] who observed that in absence of photocatalyst and under UV-irradiation, the organic compound degradation rate increases with increasing the amount of hydrogen peroxide added, but when the amount of  $H_2O_2$  (photo-Fenton effect) added exceeds certain limit, the rate of organic

compound removal becomes slightly lower than those measured in absence of photocatalyst. It was also observed by Réti et al. [58] that the performance of composites prepared from titanium decreased at extreme acidic pH because the anatase content decreased. The tested fibre is mainly composed of anatase (see below in Section 4).

### 2.8. Comparative Kinetic Study of the Degradation of the Organic Compounds Tested

Four aromatic organic compounds, phenol, 4-chlorophenol, pyrene and bisphenol A, of different chemical structure, nature and toxic to the environment were studied, in order to check if there are significant differences in their photocatalytic degradation according to their different chemical structures and degree of substitution (Figure 10).

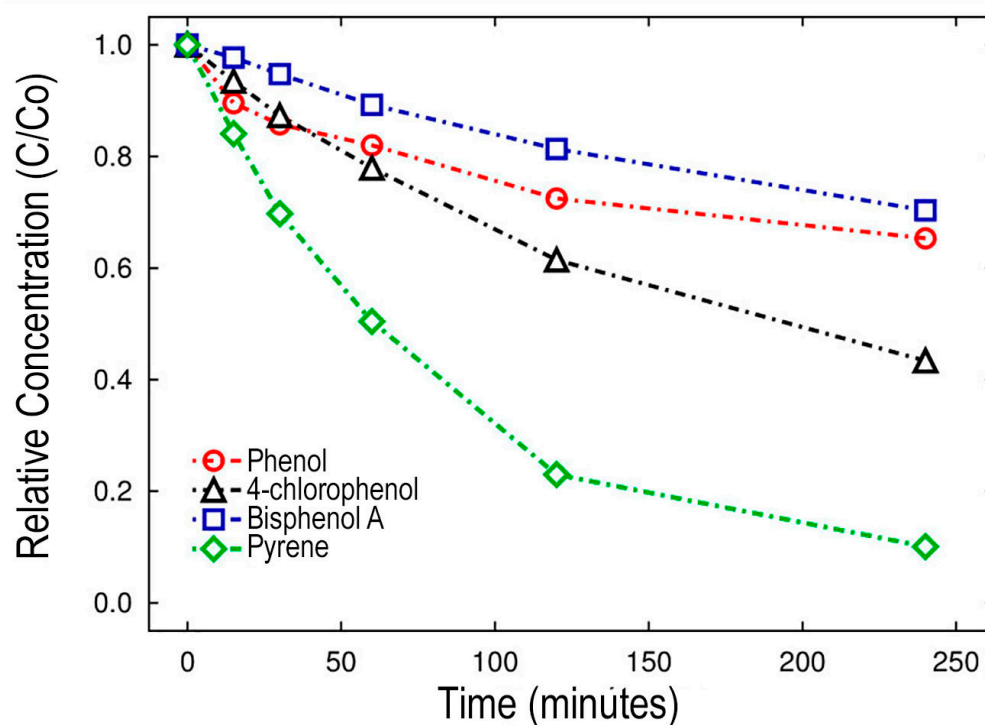


Figure 10. Photocatalytic degradation of the different compounds tested.

As can be seen in Figure 10, the photocatalytic effect at  $Q = 2000 \text{ L/h}$  and  $T = 20 \pm 1 \text{ }^\circ\text{C}$  is greater in the degradation of pyrene ( $k_{op} = 0.72 \pm 0.05 \text{ h}^{-1}$ ) than in the oxidation of the other compounds studied, which are of the same order of magnitude: 4-chlorophenol ( $k_{op} = 0.23 \pm 0.02 \text{ h}^{-1}$ ), phenol ( $k_{op} = 0.18 \pm 0.08 \text{ h}^{-1}$ ) and bisphenol A ( $k_{op} = 0.27 \pm 0.08 \text{ h}^{-1}$ ). Low operational rate constants ( $k_{op}$ ) were observed, with no differences regarding structure or degree of substitution. On the other hand, differences were observed with regard to the initial concentration of the compound to be degraded, with the lower the initial concentration the higher the  $k_{op}$  of the reaction. It has also been observed that the degradation rate follows an asymptotic behaviour due to the saturation of the catalyst surface, which suggests that an inhibition of the substrate excess type may occur.

It could be assumed that the different molecular sizes of these contaminants, their different electronic distributions, chemical groups, hydrophobicity/hydrophilicity balances, can influence their adsorption processes on the photocatalyst surface and, consequently, their photocatalytic degradation kinetics (Figure 10). However, without having carried out a detailed study of their possible degradation byproducts and pathways, it is premature to venture a rational explanation of the specific molecular causes of the greater photocatalytic degradability of pyrene compared to phenols.

Several authors have studied selective adsorption in combination with photocatalysis to improve the removal of organic compounds in water. Thus, Hitchman and Tian [59]

found similar removal rates to those found in this study for the photocatalytic degradation of 4-chlorophenol on TiO<sub>2</sub> films prepared by chemical vapour deposition (CVD) at comparable radiation times and similar initial concentrations. Dumitriu et al. [60] found low removal rates for the photocatalysis of phenol on TiO<sub>2</sub> films supported on glass by ion bombardment, similar to those found in our study. Choquette-Labbé et al. [61] also studied the degradation of phenol and derivatives using TiO<sub>2</sub> nanoparticles and Chen et al. in 2016 [62], in a study on the photocatalytic degradation of bisphenol A, also obtained similar values to those found in the present study.

### 3. Discussion

These results support the idea that the photocatalytic degradation process of the organic compounds studied is strongly influenced by the adsorption capacity of the pollutant on the surface of the catalytic fibre.

One explanation for the results obtained is that the heterogeneous phase reaction predominates over the homogeneous phase reaction. In this sense, the adsorption of the pollutants on the surface of the fibre takes place first and when the light hits the surface of the titanium dioxide, the hole-electron pair ( $h^+ / e^-$ ) is generated and forms the hydroxyl radicals ( $\bullet OH$ ), with most of these being adsorbed on the surface of the photocatalyst (heterogeneous phase) and only a small amount of the hydroxyl radicals passing to the aqueous phase (homogeneous phase). Thus, it is mainly on the fibre surface that the degradation reaction takes place and the products are formed. When the concentration of the pollutant is low, its adsorption on the surface leaves a large part of the catalyst area free for the incident ultraviolet radiation to generate the hole-electron pair ( $h^+ / e^-$ ), to form the radicals ( $\bullet OH$ ), and to carry out the degradation both heterogeneously and homogeneously. However, when the adsorption of the pollutant is very high, the entire surface of the photocatalyst is coated, preventing the ultraviolet radiation from reaching the surface, thus decreasing the number of sites available for the generation of the hollow-electron pair ( $h^+ / e^-$ ) and decreasing the photolytic reaction. This is independent of whether the reaction in the heterogeneous phase predominates over the reaction in the homogeneous phase or not, because simply, as the ( $h^+ / e^-$ ) pair is not generated, the  $\bullet OH$  radicals responsible for the degradation are not formed, producing what we could call an inhibition due to excess substrate.

### 4. Materials and Methods

#### 4.1. TiO<sub>2</sub>/SiO<sub>2</sub> Fixed Bed Photoreactor with Total Recirculation

The TiO<sub>2</sub>/SiO<sub>2</sub> fixed bed photoreactor (supplied by UBE Industries, Ltd., Tokyo, Japan) used in this work is shown in Figure 11. The system has a tank for the sample with a capacity of 200 L, a 1 hp pump for recirculation of the sample through the system, and, at the outlet of the pump, the water first goes through a 50  $\mu m$  solid filter and then through a rotameter to measure the sample flow entering the photoreactor body.

The photoreactor is characterized by maintaining a vertical piston flow with bottom inlet and upper lateral outlet; the reactor body is made of stainless steel and has a manometer on the bottom and another on the top. The internal walls of the photoreactor are polished in such a way that the radiation that reaches them is reflected, thus generating greater incidence of light on the photocatalyst.

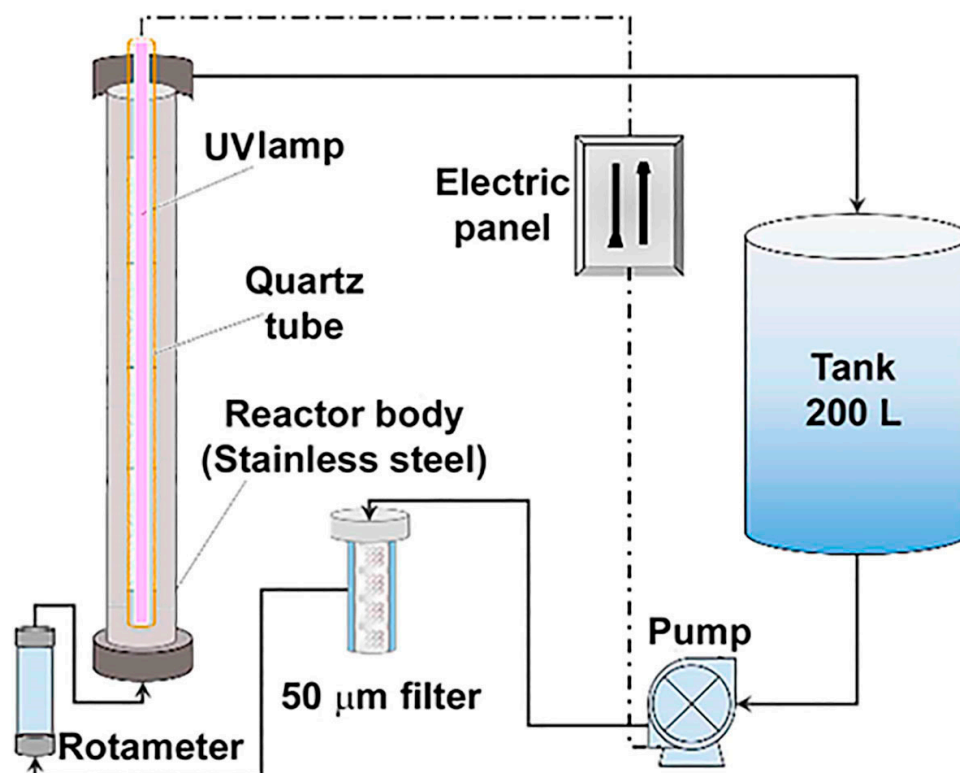


**Figure 11.** Photoreactor system used for photolytic and photocatalytic degradation processes of organic compounds.

For the photocatalysis experiments, in addition to the pilot photoreactor described, a  $\text{TiO}_2/\text{SiO}_2$  photocatalyst (UBE Industries, Ltd., Tokyo, Japan) was used. The semiconductor material used as a non-woven photocatalytic fibre with gradient in the crystalline structure, whose patent belongs to the company UBE Chemical Industries [18,19], consists of a  $\text{SiO}_2$  fibre mesh, which supports the  $\text{TiO}_2$  catalyst, generating a  $\text{TiO}_2/\text{SiO}_2$  catalyst/support system, avoiding the phenomenon of dragging of the photocatalyst from the surface of the support (a phenomenon known as peeling), as a consequence of its friction with the fluid of the liquid. The maximum pressure that the fibre can withstand is up to  $10 \text{ Kg}/\text{cm}^2$ , with optimum performance in the range of 3 to  $6 \text{ Kg}/\text{cm}^2$ . The  $\text{TiO}_2$  semiconductor is immobilized on a  $\text{SiO}_2$  fibre, contained in 4 stainless steel conical meshes placed longitudinally on rods to support them. The photocatalyst is located between the radiation source and the walls of the photoreactor [39]. Low-pressure mercury lamps were used as irradiation sources: a 40 W lamp (Philips TUV 36T5 HE 4P SE UNP/32, Amsterdam, The Netherlands), emitting 15 W of UV-C ultraviolet radiation with a maximum wavelength of 253.7 nm. The lamp was placed inside a transparent quartz tube to prevent it from coming into contact with the sample.

To study the crystalline state of the photocatalytic fibre, its X-ray diffractogram was carried out (Figure 12) and performed using a Bruker D8 Advance diffractometer (Bruker BioSpin Corporation, Billerica, MA, USA). The diffractogram shows that the fibre is formed only by  $\text{SiO}_2$  and  $\text{TiO}_2$  and, furthermore, that of the 3 crystalline varieties of  $\text{TiO}_2$ , brookite, rutile and anatase, only anatase exists in this photocatalytic fibre, with a larger surface area and a high surface density of active adsorption and surface reaction sites on the photocatalytic fibre.

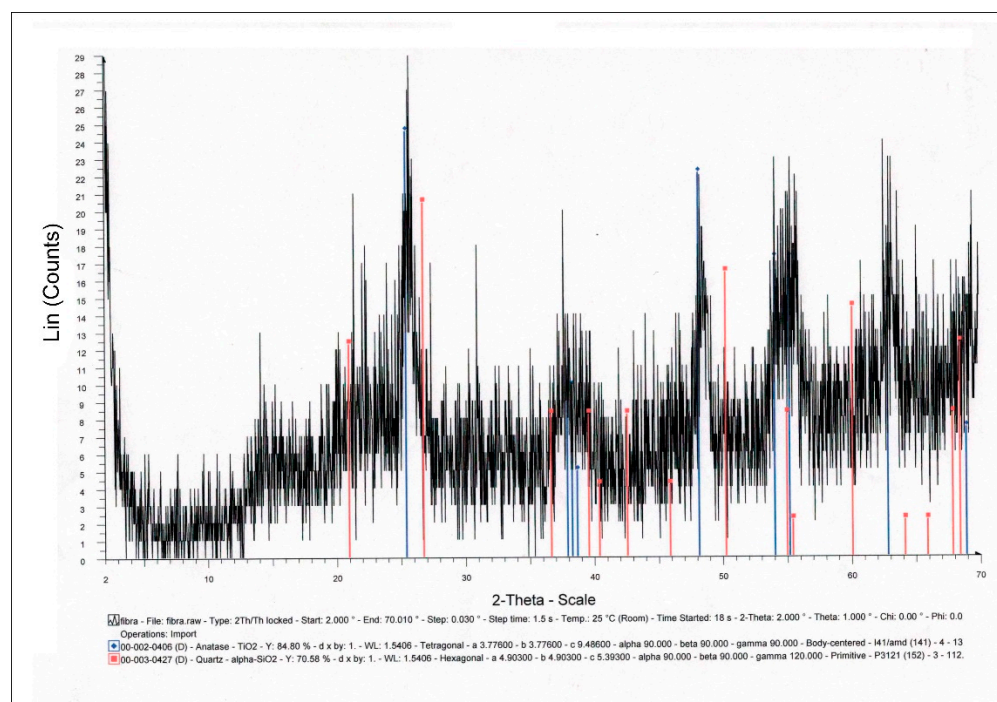


**Figure 12.** X-ray diffractogram of the UBE photocatalytic fibre.

#### 4.2. Experimental Conditions

In order to establish the experimental conditions for the study of the organic compounds degradation in the UV-C photocatalytic reactor, the following considerations were taken into account.

Synthetic wastewaters with different organic compounds concentrations similar to those existing in industrial wastewater treatment plants were used. To carry out the degradation experiments in the UBE photocatalytic plant, volumes of 50 L of aqueous solutions of each of the substances tested were used in the feed tank of the photocatalytic reactor. The pump is activated by adjusting the flow rate with the rotameter to each of the flow rates studied and the lamp is switched on. This moment is taken as time zero and aliquot samples are taken from the sample tank at specific time intervals maintaining a constant temperature, which is controlled by means of a coolant.

As organic compounds, the endocrine disruptor bisphenol A, the polycyclic aromatic compound pyrene and two phenolic compounds, 4-chlorophenol and phenol, which were supplied by Sigma-Aldrich (St. Louis, MO, USA), were chosen. For pyrene, its decomposition kinetics was followed by its fluorescence spectra using a PERKIN ELMER LS 50 fluorescence spectrometer (PerkinElmer, Inc., Waltham, MA, USA). For 4-chlorophenol, phenol and bisphenol A, the pollutant was identified by HPLC area using an Agilent-Hewlett Packard HPLC Series 1100 equipped with a Waters Spherisorb ODS3 5 m, 4 mm × 25 mm column and a diode array detector (DAD) (Agilent, Santa Clara, CA, USA).

The stability studies of the photocatalytic fibre were carried out by energy dispersive X-ray elemental microanalysis (EDXMA) on a Tecnai Spirit Twin 120 kV Transmission Electron Microscope (FEI, Hillsboro, OR, USA). This technique was also used to measure the titanium/silicon ratio of the fibre as well as the percentage of titanium on the surface fibre.

#### 4.3. Data Analysis

Free open source software has been used for the different studies. For the chemical kinetics studies of the organic compounds degradation tests and modelling of the proposed mechanism, the statistical package SIMFIT has been used. This package has been developed at the University of Manchester by Dr. William G. Bardsley (<http://www.simfit.org.uk>) (accessed on 20 November 2021). The Spanish version of SIMFIT is maintained by Dr. F. J.

Burguillo of the University of Salamanca (<http://simfit.usal.es>) (accessed on 14 December 2021) [53].

The “INRATE” program was used for the calculation of the initial rates at the different substrate concentrations. The Langmuir–Hinshelwood integrated rate equation was fitted to the appropriate model using the “QNFIT” program.

## 5. Conclusions

The performance of the photoreactor has been studied as a function of operational variables using model substances. It was found that the photocatalytic surface area plays an important role in the degradation performance of the substance. Thus, increasing the photocatalytic surface area (number of TiO<sub>2</sub> active sites) increases the degradation rate of the substrate. For compounds that are degraded simultaneously by photolytic (radiation only) and photocatalytic (radiation and photocatalytic fibre) routes, the catalyst surface area plays an essential role in the dominance of one process over the other.

This fact is corroborated by the different studies carried out, showing a high adsorption of the model substances on the surface of the photocatalyst, with high values of adsorption equilibrium constants and surface coverage, a low influence of temperature with low values of energy and enthalpy of activation and a high value of negative activation entropy, which suggests that the intermediate formed on the surface of the catalyst is more ordered than the reagents, which favours surface adsorption on the photocatalytic fibre. Similarly, the study of the pollutant contact time in the reactor has revealed that mass transfer is rate limiting at low recirculation flow rates, while surface kinetics is rate limiting at moderate flow rates. In other words, the rate of pollutant degradation increases with increasing flow rate, although this effect is reversed as residence time decreases as surface phenomena become rate limiting. This also explains the greater efficacy and efficiency in the degradation of organic compounds by photocatalytic route than by the photolytic route for those compounds that can be degraded by both routes.

Finally, the study of the stability of the fibre against acids, bases and peroxides indicates that the fibre is stable against pH, except at extreme pH, with loss of titanium at very acidic pH and loss of silicon at very basic pH. On the other hand, it is observed that the fibre is less stable against peroxides, since at high concentrations a degradation of the fibre is observed due to the loss of the active surface (titanium) of the fibre. It has been found that the dirt on the surface of the fibre containing titanium dioxide, after various experiments, does not affect the generation of hydroxyl radicals on the surface of the photocatalyst.

For these reasons, it is proposed for future works of this type that a simultaneous study of the adsorption of pollutants on the photocatalytic fibre and of the kinetics of their degradation should be carried out.

**Author Contributions:** Methodology: J.C.G.-P. and M.G.-R.; validation: J.C.G.-P. and M.G.-R.; formal analysis: J.C.G.-P. and M.G.-R.; investigation: J.C.G.-P. and M.G.-R.; resources: J.C.G.-P., M.G.-R. and J.B.P.-N.; data curation: L.A.G.-B., M.G.-R. and J.C.G.-P.; writing—original draft preparation: J.C.G.-P. and M.G.-R.; writing—review and editing: J.C.G.-P., M.G.-R. and J.B.P.-N.; visualization: J.C.G.-P. and M.G.-R.; supervision: J.C.G.-P., L.A.G.-B., M.G.-R. and J.B.P.-N.; project administration: M.G.-R.; funding acquisition: J.C.G.-P. and M.G.-R. All authors have read and agreed to the published version of the manuscript.

**Funding:** Funding: L.A.G.-B. and J.B.P.-N. thank the Consejo Nacional de Ciencia y Tecnología (CONACyT), who provided funding. They also received support from Instituto Politécnico Nacional (IPN/SIP project 20190247 and 20200670). In addition, the authors acknowledge the financial support and the supply of the photocatalytic fibre pilot plant from UBE Corporation Europe S.A. The content does not necessarily reflect the views and policies of the funding organizations.

**Data Availability Statement:** Data are contained within the article.

**Acknowledgments:** The authors wish to thank UBE Corporation Europe S.A. for supplying the photocatalytic fibre pilot plant and supporting financially this project.

**Conflicts of Interest:** The authors declare no conflict of interest.

## References

1. Chong, M.N.; Jin, B.; Chow, C.W.K.; Saint, C. Recent developments in photocatalytic water treatment technology: A review. *Water Res.* **2010**, *44*, 2997–3027. [[CrossRef](#)]
2. Ahmad, R.; Ahmad, Z.; Khan, A.U.; Mastoi, N.R.; Aslam, M.; Kim, J. Photocatalytic systems as an advanced environmental remediation: Recent developments, limitations and new avenues for applications. *J. Environ. Chem. Eng.* **2016**, *4*, 4143–4164. [[CrossRef](#)]
3. Thiruvenkatachari, R.; Vigneswaran, S.; Moon, I.S. A review on UV/TiO<sub>2</sub> photocatalytic oxidation process (Journal Review). *Korean J. Chem. Eng.* **2008**, *25*, 64–72. [[CrossRef](#)]
4. Ahmed, S.N.; Haider, W. Heterogeneous photocatalysis and its potential applications in water and wastewater treatment: A review. *Nanotechnology* **2018**, *29*, 342001. [[CrossRef](#)] [[PubMed](#)]
5. Sarkar, S.; Das, R.; Choi, H.; Bhattacharjee, C. Involvement of process parameters and various modes of application of TiO<sub>2</sub> nanoparticles in heterogeneous photocatalysis of pharmaceutical wastes—A short review. *RSC Adv.* **2014**, *4*, 57250–57266. [[CrossRef](#)]
6. Chekir, N.; Tassalit, D.; Benhabiles, O.; Merzouk, N.K.; Ghenna, M.; Abdessemed, A.; Issaadi, R. A comparative study of tartrazine degradation using UV and solar fixed bed reactors. *Int. J. Hydrogen Energy* **2017**, *42*, 8948–8954. [[CrossRef](#)]
7. Lee, C.M.; Palaniandy, P.; Dahlan, I. Pharmaceutical residues in aquatic environment and water remediation by TiO<sub>2</sub> heterogeneous photocatalysis: A review. *Environ. Earth Sci.* **2017**, *76*, 611. [[CrossRef](#)]
8. Bhatkhande, D.S.; Pangarkar, V.G.; Beenackers, A.A.C.M. Photocatalytic degradation for environmental applications—A review. *J. Chem. Technol. Biotechnol.* **2002**, *77*, 102–116. [[CrossRef](#)]
9. Hassandoost, R.; Pouran, S.R.; Khataee, A.; Orooji, Y.; Joo, S.W. Hierarchically structured ternary heterojunctions based on Ce<sup>3+</sup>/Ce<sup>4+</sup> modified Fe<sub>3</sub>O<sub>4</sub> nanoparticles anchored onto graphene oxide sheets as magnetic visible-light-active photocatalysts for decontamination of oxytetracycline. *J. Hazard. Mater.* **2019**, *376*, 200–211. [[CrossRef](#)]
10. Rao, Y.; Zhang, Y.; Li, A.; Zhang, T.; Jiao, T. Photocatalytic activity of G-TiO<sub>2</sub>@Fe<sub>3</sub>O<sub>4</sub> with persulfate for degradation of alizarin red S under visible light. *Chemosphere* **2021**, *266*, 129236. [[CrossRef](#)] [[PubMed](#)]
11. Rad, T.S.; Khataee, A.; Pouran, S.R. Synergistic enhancement in photocatalytic performance of Ce (IV) and Cr (III) co-substituted magnetite nanoparticles loaded on reduced graphene oxide sheets. *J. Colloid Interface Sci.* **2018**, *528*, 248–262. [[CrossRef](#)] [[PubMed](#)]
12. Konstantinou, I.K.; Albanis, T.A. TiO<sub>2</sub>-assisted photocatalytic degradation of azo dyes in aqueous solution: Kinetic and mechanistic investigations: A review. *Appl. Catal. B Environ.* **2004**, *49*, 1–14. [[CrossRef](#)]
13. Chen, D.; Cheng, Y.; Zhou, N.; Chen, P.; Wang, Y.; Li, K.; Huo, S.; Cheng, P.; Peng, P.; Zhang, R.; et al. Photocatalytic degradation of organic pollutants using TiO<sub>2</sub>-based photocatalysts: A review. *J. Clean. Prod.* **2020**, *268*, 121725. [[CrossRef](#)]
14. Luo, C.; Ren, X.; Dai, Z.; Zhang, Y.; Qi, X.; Pan, C. Present Perspectives of Advanced Characterization Techniques in TiO<sub>2</sub>-Based Photocatalysts. *ACS Appl. Mater. Interfaces* **2017**, *9*, 23265–23286. [[CrossRef](#)] [[PubMed](#)]
15. Chen, J.; Qiu, F.; Xu, W.; Cao, S.; Zhu, H. Recent progress in enhancing photocatalytic efficiency of TiO<sub>2</sub>-based materials. *Appl. Catal. A Gen.* **2015**, *495*, 131–140. [[CrossRef](#)]
16. Dijkstra, M.; Michorius, A.; Buwalda, H.; Panneman, H.; Winkelman, J.; Beenackers, A. Comparison of the efficiency of immobilized and suspended systems in photocatalytic degradation. *Catal. Today* **2001**, *66*, 487–494. [[CrossRef](#)]
17. Yasmina, M.; Mourad, K.; Mohammed, S.H.; Khaoula, C. Treatment Heterogeneous Photocatalysis; Factors Influencing the Photocatalytic Degradation by TiO<sub>2</sub>. *Energy Procedia* **2014**, *50*, 559–566. [[CrossRef](#)]
18. Ishikawa, T.; Yamaoka, H.; Harada, Y.; Fujii, T.; Nagasawa, T. A general process for in situ formation of functional surface layers on ceramics. *Nat. Cell Biol.* **2002**, *416*, 64–67. [[CrossRef](#)]
19. Ishikawa, T. Advances in Inorganic Fibers. *Polym. Inorg. Fibers* **2005**, *178*, 109–144. [[CrossRef](#)]
20. And, C.A.; Bard, A.J. Improved Photocatalytic Activity and Characterization of Mixed TiO<sub>2</sub>/SiO<sub>2</sub> and TiO<sub>2</sub>/Al<sub>2</sub>O<sub>3</sub> Materials. *J. Phys. Chem. B* **1997**, *101*, 2611–2616. [[CrossRef](#)]
21. Zou, L.; Luo, Y.; Hooper, M.; Hu, E. Removal of VOCs by photocatalysis process using adsorption enhanced TiO<sub>2</sub>-SiO<sub>2</sub> catalyst. *Chem. Eng. Processing Process Intensif.* **2006**, *45*, 959–964. [[CrossRef](#)]
22. Wang, C.-C.; Lee, C.-K.; Lyu, M.-D.; Juang, L.-C. Photocatalytic degradation of C.I. Basic Violet 10 using TiO<sub>2</sub> catalysts supported by Y zeolite: An investigation of the effects of operational parameters. *Dye. Pigment.* **2008**, *76*, 817–824. [[CrossRef](#)]
23. Liu, S.; Chen, X. A TiO<sub>2</sub>/AC composite photocatalyst with high activity and easy separation prepared by a hydrothermal method. *J. Hazard. Mater.* **2007**, *143*, 257–263. [[CrossRef](#)] [[PubMed](#)]
24. Kitano, M.; Matsuoka, M.; Ueshima, M.; Anpo, M. Recent developments in titanium oxide-based photocatalysts. *Appl. Catal. A Gen.* **2007**, *325*, 1–14. [[CrossRef](#)]
25. Arai, Y.; Tanaka, K.; Khlaifat, A. Photocatalysis of SiO<sub>2</sub>-loaded TiO<sub>2</sub>. *J. Mol. Catal. A Chem.* **2006**, *243*, 85–88. [[CrossRef](#)]
26. Haider, A.J.; Jameel, Z.N.; Al-Hussaini, I.H. Review on: Titanium Dioxide Applications. *Energy Procedia* **2019**, *157*, 17–29. [[CrossRef](#)]
27. Biyoghe Bi Ndong, L.; Ibondou, M.P.; Gu, X.; Lu, S.; Qiu, Z.; Sui, Q.; Mbadinga, S.M. Enhanced Photocatalytic Activity of TiO<sub>2</sub> Nanosheets by Doping with Cu for Chlorinated Solvent Pollutants Degradation. *Ind. Eng. Chem. Res.* **2014**, *53*, 1368–1376. [[CrossRef](#)]
28. Kumaresan, L.; Mahalakshmi, M.; Palanichamy, M.; Murugesan, V. Synthesis, Characterization, and Photocatalytic Activity of Sr<sup>2+</sup> Doped TiO<sub>2</sub> Nanoplates. *Ind. Eng. Chem. Res.* **2010**, *49*, 1480–1485. [[CrossRef](#)]

29. Zaleska, A. Doped-TiO<sub>2</sub>: A Review. *Recent Pat. Eng.* **2008**, *2*, 157–164. [CrossRef]
30. Fischbach, D.; Lemoine, P. Influence of a CVD carbon coating on the mechanical property stability of Nicalon SiC fiber. *Compos. Sci. Technol.* **1990**, *37*, 55–61. [CrossRef]
31. Murfin, A.; Binner, J. Thermally enhanced slip casting of alumina ceramics. *Ceram. Int.* **1998**, *24*, 597–603. [CrossRef]
32. Iwasaki, T.; Satoh, M.; Ito, T. Coating of soft metal particles with ceramic fines using a dry mechanical method. *J. Mater. Processing Technol.* **2004**, *146*, 330–337. [CrossRef]
33. Meille, V. Review on methods to deposit catalysts on structured surfaces. *Appl. Catal. A Gen.* **2006**, *315*, 1–17. [CrossRef]
34. Braham, R.J.; Harris, A.T. Review of Major Design and Scale-up Considerations for Solar Photocatalytic Reactors. *Ind. Eng. Chem. Res.* **2009**, *48*, 8890–8905. [CrossRef]
35. Cassano, A.E.; Alfano, O.M. Reaction engineering of suspended solid heterogeneous photocatalytic reactors. *Catal. Today* **2000**, *58*, 167–197. [CrossRef]
36. Tokode, O.; Prabhu, R.; Lawton, L.A.; Robertson, P.K.J. UV LED Sources for Heterogeneous Photocatalysis. In *The Handbook of Environmental Chemistry Part III*; Bahnemann, D., Robertson, P., Eds.; Springer: Berlin/Heidelberg, Germany, 2014; Volume 35, pp. 159–179. [CrossRef]
37. Rodríguez, S.M.; Richter, C.; Galvez, J.B.; Vincent, M. Photocatalytic degradation of industrial residual waters. *Sol. Energy* **1996**, *56*, 401–410. [CrossRef]
38. Ou, Y.; Lin, J.; Fang, S.; Liao, D. Study on the preparation of ultrafine mesoporous TiO<sub>2</sub> with controllable crystalline phase and its photocatalytic activities. *Catal. Commun.* **2007**, *8*, 936–940. [CrossRef]
39. Cachaza Silverio, J.; Diez Mateos, A.; García-Prieto, J.C. La fotocatalisis como tecnología para la desinfección del agua sin aditivos químicos. Ensayos del reactor fotocatalítico UBE en la inactivación de microorganismos. *Rev. Tecnol. Agua* **2005**, *261*, 81–85.
40. De Felipe-García, F. Instalación de fotocatalizador para desinfectar el agua de la torre de refrigeración en la clínica La Luz de Madrid. *Montajes Instal.* **2008**, *10*, 78–82.
41. Pantoja-Espinosa, J.C.; Proal-Nájera, J.B.; García-Roig, M.; Chairez-Hernández, I.; Osorio-Revilla, G.I. Eficiencias comparativas de inactivación de bacterias coliformes en efluentes municipales por fotólisis (UV) y por fotocatalisis (UV/TiO<sub>2</sub>/SiO<sub>2</sub>). Caso: Depuradora de aguas de Salamanca, España. *Rev. Mex. Ing. Química* **2015**, *14*, 119–135.
42. Núñez-Núñez, C.M.; Chairez-Hernández, I.; García-Roig, M.; García-Prieto, J.C.; Melgoza-Alemán, R.M.; Proal-Nájera, J.B. UV-C/H<sub>2</sub>O<sub>2</sub> heterogeneous photocatalytic inactivation of coliforms in municipal wastewater in a TiO<sub>2</sub>/SiO<sub>2</sub> fixed bed reactor: A kinetic and statistical approach. *React. Kinet. Mech. Catal.* **2018**, *125*, 1159–1177. [CrossRef]
43. González-Burciaga, L.; García-Prieto, J.; García-Roig, M.; Lares-Asef, I.; Núñez-Núñez, C.; Proal-Nájera, J. Cytostatic Drug 6-Mercaptopurine Degradation on Pilot Scale Reactors by Advanced Oxidation Processes: UV-C/H<sub>2</sub>O<sub>2</sub> and UV-C/TiO<sub>2</sub>/H<sub>2</sub>O<sub>2</sub> Kinetics. *Catalysts* **2021**, *11*, 567. [CrossRef]
44. Adán, C.; Coronado, J.M.; Bellod, R.; Soria, J.; Yamaoka, H. Photochemical and photocatalytic degradation of salicylic acid with hydrogen peroxide over TiO<sub>2</sub>/SiO<sub>2</sub> fibres. *Appl. Catal. A Gen.* **2006**, *303*, 199–206. [CrossRef]
45. Liu, Y.; Yu, H.; Lv, Z.; Zhan, S.; Yang, J.; Peng, X.; Ren, Y.; Wu, X. Simulated-sunlight-activated photocatalysis of Methylene Blue using cerium-doped SiO<sub>2</sub>/TiO<sub>2</sub> nanostructured fibers. *J. Environ. Sci.* **2012**, *24*, 1867–1875. [CrossRef]
46. Belgiorno, V.; Rizzo, L.; Fatta-Kassinos, D.; Della Rocca, C.; Lofrano, G.; Nikolaou, A.; Naddeo, V.; Meric, S. Review on endocrine disrupting-emerging compounds in urban wastewater: Occurrence and removal by photocatalysis and ultrasonic irradiation for wastewater reuse. *Desalination* **2007**, *215*, 166–176. [CrossRef]
47. Directive on Environmental Quality Standards (Directive 2008/105/EC) (EQSD). Available online: <https://eur-lex.europa.eu/legal-content/EN/TXT/?uri=CELEX:32008L0105> (accessed on 10 December 2021).
48. Kumar, K.V.; Porkodi, K.; Rocha, F. Langmuir–Hinshelwood kinetics—A theoretical study. *Catal. Commun.* **2008**, *9*, 82–84. [CrossRef]
49. Herrmann, J.-M. Heterogeneous photocatalysis: Fundamentals and applications to the removal of various types of aqueous pollutants. *Catal. Today* **1999**, *53*, 115–129. [CrossRef]
50. Fernández Ibáñez, P. Propiedades Coloidales de Partículas de TiO<sub>2</sub>: Aplicación al Tratamiento Fotocatalítico Solar de Aguas. Ph.D. Thesis, University of Granada, Granada, Spain, 2003.
51. Rayne, S.; Forest, K.; Friesen, K.J. Mechanistic aspects regarding the direct aqueous environmental photochemistry of phenol and its simple halogenated derivatives. A review. *Environ. Int.* **2009**, *35*, 425–437. [CrossRef]
52. Hoffmann, M.R.; Martin, S.T.; Choi, W.; Bahnemann, D.W. Environmental Applications of Semiconductor Photocatalysis. *Chem. Rev.* **1995**, *95*, 69–96. [CrossRef]
53. Bardsley, W.G. Simfit Statistical package. v. 7.3.1 Academic 64-bit. University of Manchester, UK. Available online: <http://www.simfit.man.ac.uk> (accessed on 14 December 2021).
54. Fox, M.A.; Dulay, M.T. Heterogeneous photocatalysis. *Chem. Rev.* **1993**, *93*, 341–357. [CrossRef]
55. Gálvez, J.B.; Rodríguez, S.M.; Gasca, C.A.E.; Bandala, E.R.; Gelover, S.; Leal, T. Purificación de aguas por fotocatalisis heterogénea: Estado del arte. *Academia*. 2001. Available online: [https://www.academia.edu/16138640/Purificaci%C3%B3n\\_de\\_aguas\\_por\\_fotocat%C3%A1lisis\\_heterog%C3%A9nea\\_estado\\_del\\_arte?from=cover\\_page](https://www.academia.edu/16138640/Purificaci%C3%B3n_de_aguas_por_fotocat%C3%A1lisis_heterog%C3%A9nea_estado_del_arte?from=cover_page) (accessed on 10 December 2021).
56. Gaya, U.I.; Abdullah, A.H. Heterogeneous photocatalytic degradation of organic contaminants over titanium dioxide: A review of fundamentals, progress and problems. *J. Photochem. Photobiol. C Photochem. Rev.* **2008**, *9*, 1–12. [CrossRef]

57. AENOR Internacional, S.A.U. Products Used for Treatment of Water Intended for Human Consumption—Inorganic Supporting and Filtering Materials—Methods of Test. AENOR. In CALIDAD DEL AGUA, 4.<sup>a</sup> EDICIÓN. CD-ROM 2009 Ed. ISBN 9788481436365. Available online: <https://www.agapea.com/libros/Calidad-del-agua-4-edicion-CD-ROM-9788481436365-i.htm> (accessed on 14 December 2021).
58. Réti, B.; Major, Z.; Szarka, D.; Boldizsár, T.; Horváth, E.; Magrez, A.; Forró, L.; Dombi, A.; Hernádi, K. Influence of TiO<sub>2</sub> phase composition on the photocatalytic activity of TiO<sub>2</sub>/MWCNT composites prepared by combined sol–gel/hydrothermal method. *J. Mol. Catal. A Chem.* **2016**, *414*, 140–147. [[CrossRef](#)]
59. Hitchman, M.L.; Tian, F. Studies of TiO<sub>2</sub> thin films prepared by chemical vapour deposition for photocatalytic and photoelectrocatalytic degradation of 4-chlorophenol. *J. Electroanal. Chem.* **2002**, *538–539*, 165–172. [[CrossRef](#)]
60. Dumitriu, D.; Bally, A.; Ballif, C.; Hones, P.; Schmid, P.; Sanjinés, R.; Lévy, F.; Pârvulescu, V. Photocatalytic degradation of phenol by TiO<sub>2</sub> thin films prepared by sputtering. *Appl. Catal. B Environ.* **2000**, *25*, 83–92. [[CrossRef](#)]
61. Choquette-Labbé, M.; Shewa, W.A.; Lalman, J.A.; Shanmugam, S.R. Photocatalytic Degradation of Phenol and Phenol Derivatives Using a Nano-TiO<sub>2</sub> Catalyst: Integrating Quantitative and Qualitative Factors Using Response Surface Methodology. *Water* **2014**, *6*, 1785–1806. [[CrossRef](#)]
62. Chen, P.-J.; Linden, K.G.; Hinton, D.E.; Kashiwada, S.; Rosenfeldt, E.J.; Kullman, S.W. Biological assessment of bisphenol A degradation in water following direct photolysis and UV advanced oxidation. *Chemosphere* **2006**, *65*, 1094–1102. [[CrossRef](#)] [[PubMed](#)]